Observation of Coherent Sheared Turbulence Flows in the DIII-D Tokamak

M. Jakubowski, R. J. Fonck, and G. R. McKee
University of Wisconsin–Madison, 1500 Engineering Drive, Madison, Wisconsin 53706-1687
(Received 1 October 2001; published 9 December 2002)

Time-resolved measurements of the turbulent density flow field in a tokamak plasma reveal low-frequency (~15 KHz), coherent oscillations in the poloidal flow, $\tilde{\boldsymbol{v}}_\theta$. These flow oscillations have a long poloidal wavelength ($m < 3$) and narrow radial extent ($k_r\rho_i \sim 0.2$). The estimated flow-shearing rate is of the same order of magnitude as the turbulence decorrelation rate and may thus regulate the turbulence amplitude. These features are consistent with theoretically predicted axisymmetric, self-regulating, sheared flows recognized as geodesic acoustic modes.

DOI: 10.1103/PhysRevLett.89.265003 PACS numbers: 52.35.Ra, 47.27.Ak, 52.25.Fi, 52.55.Fa

Developing a predictive understanding of turbulence in magnetically confined plasmas continues to be a primary challenge in controlled thermonuclear fusion research. Turbulence manifests itself as microscopic fluctuations in plasma parameters such as density ($\tilde{n}$), temperature, and electrostatic potential ($\tilde{\phi}$), and it leads to anomalously high levels of particle and energy leakage across the confining magnetic fields.

Recent theoretical work indicates that turbulence in a toroidal plasma may exist in a self-organized state mediated by axisymmetric ($n = 0$), self-generated, fluctuating, $m = 0$ poloidal $\mathbf{E} \times \mathbf{B}$ flows [1–4]. These flows, instances of which include low-frequency zonal flows ($\omega \sim 0$), or the related higher-frequency geodesic acoustic modes (GAMs) ($\omega \sim c_s/R$), are driven by fluctuations in the plasma density, potential, and temperature. Zonal flows are generated via the Reynolds stress, a coupling of radial and poloidal velocity fluctuations [1], while GAMs can be generated through a coupling of finite pressure perturbations to the toroidal magnetic geometry [4]. These flows can regulate the microinstabilities in turn through a flow shear stabilization mechanism, thereby moderating the turbulence-induced transport [5].

Given the central role attributed to these self-generated, sheared flows in establishing the steady state of turbulence and the cross-field transport rates due to this turbulence, there is considerable interest in observing features of such flows in high temperature plasmas. Experiments addressing this problem to date have examined features of the density turbulence or potential measurements in the plasma edge and scrape-off region to infer the presence of zonal flows or GAMs in tokamak plasmas [6–9] and lower-temperature heliac plasmas [10].

Direct experimental evidence of self-regulating, sheared flows and their generation mechanism requires the measurement of the turbulent velocity fields or electric potential [3]. They occur mainly in the poloidal $\mathbf{E} \times \mathbf{B}$ flow and are generally expected to be manifested less strongly in the density field (i.e., $\tilde{n}/n < \tilde{\phi}/\phi$). This calls for measurement of the flow velocity fluctuations as a means of direct experimental observation. We report here the first direct evidence of sheared flow characteristics in the poloidal flow field of the density turbulence $\tilde{\boldsymbol{v}}_\theta$ in the confined region of high temperature plasmas with fully developed turbulence.

In this work, measurements of poloidal flow-field fluctuations are derived from time-delay-estimation analysis of local density turbulence. Density turbulence is measured in the DIII-D tokamak using beam emission spectroscopy (BES) [11]. BES was developed to measure localized, long-wavelength ($k_r\rho_i < 1$, where ρ_i is the ion gyroradius) density fluctuations in high temperature tokamak plasmas through collisionally induced neutral beam fluorescence [12]. For this experiment, BES is deployed on DIII-D to measure density fluctuations at 32 spatial locations on a 5 by 6 cm grid in the outer midplane ($0.85 \leq r/a \leq 1$) of the poloidal cross section of the plasma [13].

This local $\tilde{n}(R, z, t)$ data is used to extract local velocity fluctuations through time-delay-estimation (TDE) analysis, which derives a time-varying delay between two spatially separated channels [14,15]. Measurement of given density fluctuation eddy displacement, via time delays short compared to the density fluctuation decorrelation time (~ 6–9 μs), then gives the time-dependent density fluctuation eddy velocity directly. In effect, TDE analysis is used to map the movement of particular turbulent density fluctuation structures between two observation points on turbulence-relevant time scales. The extraction of the time-varying time delay between two measurements of density fluctuations separated in the poloidal direction then gives measurements of $\tilde{\boldsymbol{v}}_\theta$. This work demonstrates the first application of this analysis technique to density fluctuation data in tokamak plasmas.

The measured $\tilde{\boldsymbol{v}}_\theta(t)$ is essentially the group velocity of the turbulence in the laboratory frame, and it is comprised of a superposition of steady-state and time-dependent $\mathbf{E}_r \times \mathbf{B}_T$ flows, plus any intrinsic mode velocity in the plasma frame. Comparisons with the $\mathbf{E} \times \mathbf{B}$ velocity inferred from charge exchange recombination measurements indicate that 50%–80% of the steady-state poloidal flow obtained via TDE analysis can be attributed

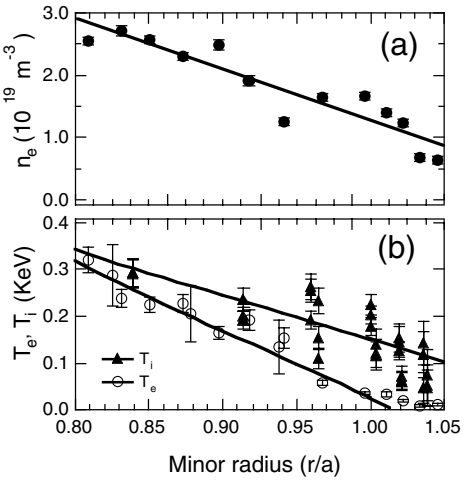

FIG. 1. Edge profiles of (a) electron density and (b) electron and ion temperatures.

to local $\mathbf{E} \times \mathbf{B}$ movement. Thus, the measured $\tilde{\boldsymbol{v}}_\theta(t)$ should manifest any contributions from a time-varying $\mathbf{E} \times \mathbf{B}$ flow, such as that resulting from a zonal flow. Note that the measured eddy flow field in the poloidal direction is not necessarily equal to the bulk mass flow of the plasma.

Application of this technique to discern the underlying turbulence flow field requires that the turbulence eddy structures being tracked persist on a time scale longer than the interchannel transit time. This condition is satisfied for the measurements presented here. The equilibrium flows are about 4–5 km/s, resulting in a 2–2.5 μs average transit time τ_d across the 1 cm channel separation in the poloidal direction. The eddy decorrelation times are approximately $\tau_c \approx 6$–9 μs, so that $\tau_c > \tau_d$. The density eddies thus effectively function as test particles to map the turbulence flow field. Furthermore, the poloidal correlation length of the density fluctuation turbulence is about 3 cm under these conditions, so that the eddy structure is well resolved with the 1 cm spatial resolution and channel spacing of the BES optical system.

Two time-varying TDE techniques are employed to measure the movement of turbulent structures between spatially separated sample points in the plasma. The first uses a time-shifted maximum overlap method, whereby a minimum difference between signals is calculated by appropriately shifting one signal in time with respect to the other [14]. The second employs a wavelet-based time-resolved correlation analysis, which was developed for the present application [15]. Improved noise characteristics are obtained at low frequency using the shift-overlap TDE method, while the wavelet approach provides wider frequency response. Both techniques yield equivalent results for the features discussed here.

TDE analysis has been applied to local density fluctuation measurements on the DIII-D tokamak. L-mode plasmas ($R = 1.73$ m, $a = 0.6$ m, $\kappa = 1.8$, $B_T = -2.0$ T, $I_p = 1.2$ MA, $P_{\text{inj}} = 5$ MW, $n_e = 3 \times 10^{19}$ m^{-3}, $kT_{i,0} \sim$ 4 keV, $q_{95} = 4.8$) were used in this first study, and the $\tilde{\boldsymbol{n}}(R, z, t)$ measurements were made in the outer plasma region to maximize the signal to noise in extracted $\tilde{\boldsymbol{v}}_\theta$. Profiles of basic plasma parameters are shown in Fig. 1, showing moderate to strong density and temperature gradients in this outer region of the plasma. Table I lists several relevant dimensionless parameters evaluated locally at $r/a = 0.85$, 0.9, and 0.95.

TABLE I. Dimensionless parameters in the experimentally observed region.

	$r/a = 0.85$	$r/a = 0.90$	$r/a = 0.95$
ν^*	0.5	0.7	1.6
ρ^* (10^{-3})	1.4	1.2	0.9
T_e/T_i	0.8	0.7	0.5
η_i	1.4	1.3	1.1
q	3.4	4.0	4.8
$\hat{\mathbf{s}}$	3.0	4.7	7.5
$\tilde{n}/n$ (%)	2	5	5

Figure 2 shows examples of the coherency, or normalized cross power, spectra for density fluctuations and $\tilde{\boldsymbol{v}}_\theta$ obtained between poloidally adjacent spatial volumes near the plasma edge region. The coherency is plotted here to emphasize the low-frequency coherent flow features. Since adjacent points in space are well within the turbulence correlation lengths, these coherency spectra show the regions of correlated turbulence power with the contributions from incoherent detector and amplifier noise suppressed.

Figure 2 shows that the density and velocity coherency spectra exist over a similar frequency range but are quite distinct from each other, and, in particular, a distinct, low-frequency feature is found only in the $\tilde{\boldsymbol{v}}_\theta$ spectrum. The density fluctuation and $\tilde{\boldsymbol{v}}_\theta$ fields are found to be uncorrelated [i.e., $\langle \tilde{\boldsymbol{n}}(f) \tilde{\boldsymbol{v}}_\theta(f) \rangle = 0$] for all frequencies even though the velocities are extracted from analysis of the density fluctuation measurements. This is also evident

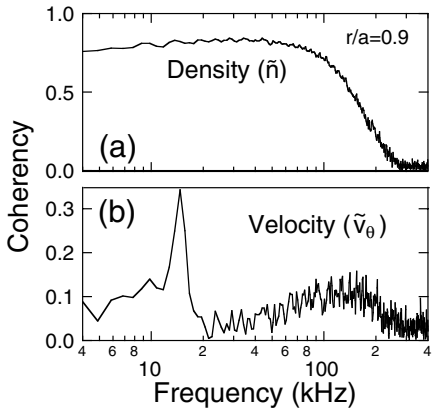

FIG. 2. Coherency spectra between adjacent spatial channels ($\Delta z = 1.1$ cm) for (a) density and (b) poloidal velocity fluctuations.

from time evolution waveforms in the sense that the $\tilde{n}(t)$ and $\tilde{v}_\theta(t)$ are dissimilar. The density fluctuation coherency spectrum shows a monotonic decay over a wide frequency range, which is typically found in the outer regions of the confined plasma. In contrast, the $\tilde{v}_\theta$ spectrum shows a distinct peaked feature at 15 kHz and a broadband component extending to $f \leq 250$ kHz.

The semicoherent low-frequency feature in the $\tilde{v}_\theta$ spectrum is noteworthy in that it suggests a long-lived, nearly coherent poloidal flow oscillation. A small but finite ($\tilde{n}/n \approx 0.2\% \ll \tilde{v}_\theta/v_{\theta,\mathrm{eq}} \approx 10\%$) density fluctuation component associated with the 15 kHz feature is observed at $r/a = 0.8$–0.85. This density fluctuation component is not observed further out radially ($0.87 < r/a < 1.0$), as seen in Fig. 2(a). The coherent feature near 15 kHz is visible in the outer plasma region, $r/a = 0.85$ to 0.96, where relatively steep gradients occur. The innermost limit for detection of this feature is set by the noise level in the density fluctuation signals and the resulting propagation of noise through the TDE analysis.

We note that this 15 kHz feature is not related to any magnetohydrodynamic (MHD) activity. There is very little MHD behavior in these discharges, and none with the frequency and temporal behavior of the observed turbulence poloidal flow fluctuation.

Comparison of the $\tilde{v}_\theta$ coherency spectra at increasing poloidal separation at $r/a = 0.89$, shown in Fig. 3, indicates that the distinctive low-frequency structure has a long correlation length in the poloidal direction, much greater than that of the density fluctuations. Also, the $\tilde{v}_\theta$ amplitude is found to be essentially constant over 4 cm, the maximum range allowed by the viewing geometry.

The higher-frequency broadband turbulence observed at $\Delta z = 1.1$ cm (Fig. 3) indicates the presence of localized, broadband turbulence in the $\tilde{v}_\theta$ field. This 20–250 kHz broadband $\tilde{v}_\theta$ component is observed to have a poloidal correlation length <2 cm, indicating a short wavelength broadband structure, similar to that found in density fluctuations, and superimposed on the 15 kHz feature.

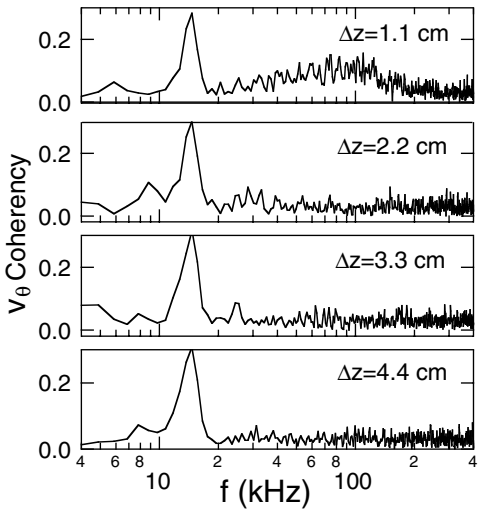

FIG. 3. Coherency spectra in $\tilde{v}_\theta$ for increasing poloidal separation between sampled volumes at $r/a = 0.9$.

Figure 4 shows the cross phase between measurements of $\tilde{v}_\theta$ for poloidal separations up to 4.4 cm. The cross phase is <0.1 rad over this range, and a linear fit to these values indicates a poloidal mode number of $m < 3$ under the assumption of a poloidally uniform perturbation of the form $\tilde{v} = \tilde{v}_0 \sin(m\theta)$.

Differences between the low-frequency peak in $\tilde{v}_\theta$ and the density fluctuation field $\tilde{n}$ in the same frequency range become evident in a comparison of their spatial and temporal correlation properties. The lifetime of the 10–20 kHz feature in $\tilde{v}_\theta$ is $\sim 200\ \mu$s as estimated from the frequency width of the peak. In contrast, the decorrelation time of the corresponding 10–20 kHz region in density fluctuations at $r/a = 0.90$ is 18 μs as measured by the temporal decay of the peak correlation envelope function with channel separation [12]. It is $\sim 10\ \mu$s for the entire frequency range. Both measures are much shorter than that of the coherent poloidal flow feature.

The spatial correlation coefficients at zero time delay are shown in Fig. 5(a) for both the density and poloidal velocity fluctuations over the 10–20 kHz frequency range and for a poloidal viewing array of six points spanning $\Delta z = 0$ to 5.6 cm at $r/a = 0.91$. The spatial correlation function for $\tilde{v}_\theta$ reveals a long, nondecaying spatial structure in the poloidal direction due to the semicoherent 15 kHz structure. This is in sharp contrast to the density fluctuation correlation function, which exhibits a typical decaying wavelike structure [12] with an overall correlation length of $L_{c,n} \sim 3$ cm for the same frequency range and ~ 2.2 cm over the entire spectrum.

Radial correlations of $\tilde{v}_\theta(f)$ are obtained by measuring the poloidal velocity fluctuations as a function of radius. The resulting radial correlation function of $\tilde{v}_\theta$ at zero time delay is shown in Fig. 5(b). In contrast to the long correlation length in the poloidal direction,

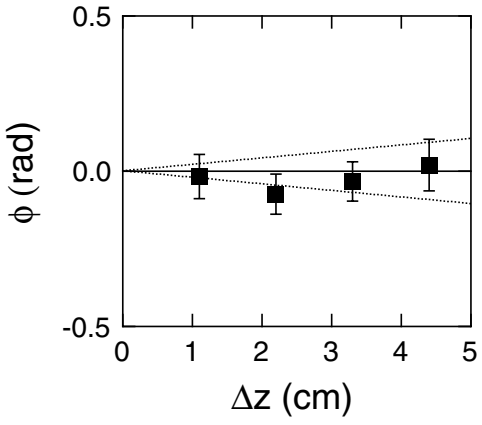

FIG. 4. Phase shift of the semicoherent 15 kHz $\tilde{v}_\theta$ feature as a function of poloidal separation in the range $0.86 \leq r/a \leq 0.95$. Lines indicate $m = \pm 2$ for reference.

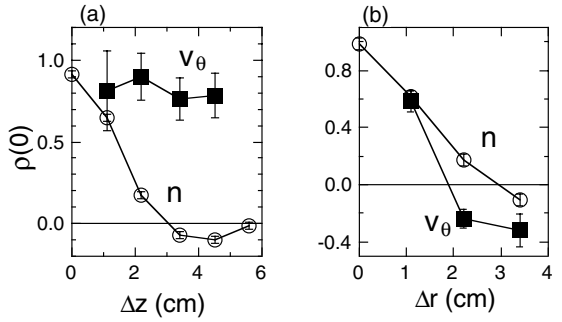

FIG. 5. Poloidal (a) and radial (b) correlation functions of $\tilde{v}_\theta$ and density fluctuations in the 10–20 kHz range.

the radial correlation length of $\tilde{v}_\theta$ is relatively short, $L_{c,v_\theta} \approx 3.3$ cm. This is comparable to the $L_{c,\tilde{n}} \approx 2.3$ cm radial correlation length of the density fluctuation field over 10–20 kHz. The density spatial structure decays mostly monotonically, while the poloidal velocity fluctuation exhibits a stronger wavelike structure, possibly with a long tail, as seen in Fig. 5(b). The radial correlation length of $\tilde{v}_\theta$ gives $k_r\rho_i = 2\pi\rho_i/L_{c,v_\theta} \approx 0.2$.

The instantaneous poloidal flow rms amplitude, normalized to the ion thermal velocity ($v_{ti} \sim 180$ km/s) is $\tilde{v}_\theta/v_{ti} \sim 0.5\%$, or $\tilde{v}_\theta/v_{\rm eq} \sim 10\%$, at $r/a = 0.91$ for the semicoherent feature in the 10–20 kHz region. For comparison, the frequency-integrated (3–300 kHz) normalized density fluctuation is $\tilde{n}/n \sim 5\%$.

The rms magnitude of the coherent poloidal flow oscillation can be used to infer a turbulence shearing rate due to this poloidal flow structure. Taking the shearing rate to be approximately $\omega_s = d\tilde{v}/dr \approx \tilde{v}_\theta/L_r$, where L_r is the radial correlation length of the $\tilde{v}_\theta$ field, we find $\omega_s \approx 5 \times 10^4$ s^{-1}. This is comparable to the inverse of the density turbulence decorrelation time, $\gamma \sim 12 \times 10^4$ s^{-1}, which to some degree can be taken as an estimate of the growth rate. The estimated shearing and growth rates are thus comparable, suggesting that the observed flows are of sufficient amplitude to alter the magnitude of the turbulence and thereby the resulting transport.

Finally, we note that the semicoherent velocity feature is observed reproducibly as a robust feature of the near-edge turbulence over a range of L-mode plasma conditions. The specific data shown here were obtained from two representative L-mode discharges.

Nonlinear turbulence simulations [3,4] have identified distinguishing features of zonal flows and GAMs which are similar to the observations reported herein. The simulations indicate that these self-generated, $m = 0$, sheared flows are radially localized ($k_r\rho_i = 0.1$–0.6), and it is just this radially localized poloidal flow that can shear eddies and thereby mediate the turbulence magnitude.

Specifically, simulations of ion-temperature-gradient driven turbulence in the edge to core transitional region [4] using a 3D Braginskii model predict poloidal flow features similar to those observed here. The model exhibits a nearly coherent $\mathbf{E} \times \mathbf{B}$ flow in spatial locations and at plasma parameters similar to those examined for this experimental study. The poloidal flows observed in this model are the geodesic acoustic modes, which here are oscillations resulting from poloidal rotation coupling to an $(m, n) = (1, 0)$ pressure perturbation by an inhomogeneous magnetic field. The small density perturbation observed at $r/a < 0.87$ might be explained by the coupling of a GAM $\mathbf{E} \times \mathbf{B}$ flow oscillation to a pressure (and therefore density) perturbation. GAMs exhibit a semicoherent temporal behavior (spectral width 5% of the eigenfrequency) and are radially localized. Of particular note is that the frequency of such a mode is predicted to be $f \sim \omega/2\pi \sim v_{T_i}/2\pi R \sim 13$ KHz for this region of the plasma (with $T_i \approx 250$ eV near $r/a = 0.9$). This is very close to the experimentally observed mode frequency of about 15 KHz. As such, the GAM frequency, $\omega_{\rm GAM} \ll \omega_{\rm turbulence}$, is sufficiently low to mediate transport [3,4]. The predicted frequency is dependent on modification factors of order unity that depend on magnetic geometry and electron to ion temperature ratio.

The features of the observed $\tilde{v}_\theta$ turbulence flow field are thus consistent with the theoretical picture of long-wavelength, radially localized shear flows and show particularly significant agreement with predictions for GAMs. These features include its frequency, spatial structure, and radial localization.

The authors thank K. Burrell, P. Diamond, T. S. Hahm, K. Hallatschek, W. Nevins, P. Terry, G. Tynan, and M. Zarnstorff for helpful discussions and suggestions. They also thank the DIII-D team for help in these experiments. This work was supported by U.S. Department of Energy Grant No. DE-FG02-89ER53296 in collaboration with the DIII-D National Fusion Facility, under Contract No. DE-AC03-99ER54463.

[1] P. H. Diamond *et al.*, *Proceedings of the 17th IAEA Fusion Energy Conference, Yokohama, 1998* (IAEA, Vienna, 2001).
[2] Z. Lin *et al.*, Science **281**, 1835 (1998).
[3] T. S. Hahm *et al.*, Plasma Phys. Control. Fusion **42**, A205 (2000).
[4] K. Hallatschek and D. Biskamp, Phys. Rev. Lett. **86**, 1223 (2001).
[5] K. H. Burrell, Science **281**, 1816 (1998).
[6] S. Coda, M. Porkolab, and K. H. Burrell, Phys. Rev. Lett. **86**, 4835 (2001).
[7] G. R. Tynan *et al.*, Phys. Plasmas **8**, 2691 (2001).
[8] R. A. Moyer *et al.*, Phys. Rev. Lett. **87**, 135001 (2001).
[9] Y. H. Xu *et al.*, Phys. Rev. Lett. **84**, 3867 (2000).
[10] M. G. Shats and W. M. Solomon, Phys. Rev. Lett. **88**, 045001 (2002).
[11] G. McKee *et al.*, Rev. Sci. Instrum. **70**, 913 (1999).
[12] R. J. Fonck *et al.*, Phys. Rev. Lett. **70**, 3736 (1993).
[13] C. Fenzi *et al.*, Rev. Sci. Instrum. **72**, 988 (2001).
[14] H. C. So, Electron. Lett. **34**, 722 (1998).
[15] M. Jakubowski *et al.*, Rev. Sci. Instrum. **72**, 996 (2001).